Aptamer-Controlled Biofuel Cells in Logic Systems and Used as Self-Powered and Intelligent Logic Aptasensors

Ming Zhou, Yan Du, Chaogui Chen, Bingling Li, Dan Wen, Shaojun Dong,* and Erkang Wang*

State Key Laboratory of Electroanalytical Chemistry, Changchun Institute of Applied Chemistry, Chinese Academy of Sciences, Changchun 130022, People's Republic of China

Received December 17, 2009; E-mail: dongsj@ciac.jl.cn; ekwang@ciac.jl.cn

Biofuel cells (BFCs) based on enzymes[1] and microbes[2] have been recently paid considerable attention because they are recognized as a new kind of energy conversion technology that possesses striking properties, such as the ability to operate under mild conditions (i.e., ambient temperature and neutral pH)[1a,b] and the potential to be used as in vivo power sources for bioelectronics, including micropumps, pacemakers, neuromorphic circuits, etc.[1a,b] In addition to major research activity relating to long-term operation, miniaturization, and power efficiency of BFCs,[1] some interesting results were recently reported for BFCs with power release logically controlled by biochemical computing (i.e., biocomputing).[3] Biocomputing, which belongs to a subarea of unconventional chemical computing and is performed by living organisms (e.g., DNA[4] and proteins/enzymes[5]), is aimed at information processing using biochemical means. Because of the highly specific catalytic or recognition reactions designed by nature, biocomputing can easily solve the interference limitation of chemical computing resulting from the incompatibility in most chemical systems.[4,5]

Aptamers, which are novel artificially selected functional DNA or RNA oligonucleotides, possess high recognition ability to a broad range of specific targets ranging from proteins to peptides, amino acids, drugs, metal ions, and even whole cells.[6] Because of their unique characteristics (e.g., versatility, specificity, and synthetic nature), aptamers exhibit many unprecedented advantages compared with antibodies or other biomimetic receptors, including a wide range of targets, comparable or even better target affinity, easy and cost-effective synthesis with high reproducibility and purity, simple and straightforward chemical modification, etc.[6] Thus, aptamers can be considered as a potential alternative to antibodies or other biomimetic receptors for the development of biotechnology, diagnostics, and therapy.[6]

In this communication, we describe the first example of controlled power release of BFCs by aptamer-based biochemical signals processed according to the Boolean logic operations "programmed" into biocomputing systems. In addition, through the built-in **NAND** logic gate, the fabricated BFCs controlled by aptamer logic systems enabled us to construct self-powered and intelligent logic aptasensors that can determine whether the two specific targets are both present in a sample. To the best of our knowledge, such "mutual benefits" between aptamers and BFCs, i.e., utilizing aptamer-based biochemical signals in a logic operation for controlling BFCs' power release and applying BFCs as biosensors for aptasensing, have not been reported to date. Their application might not only significantly increase the versatility of aptamer-based biocomputing systems, resulting in very specific responses to a large variety of biochemical signals, but also greatly enhance the adaptability of aptamer target recognition to future self-powered and intelligent logic aptasensors or related bioelectronic devices.

Scheme 1. Schematic Representation of the Components of the On-Chip BFC Controlled by an Aptamer Logic System
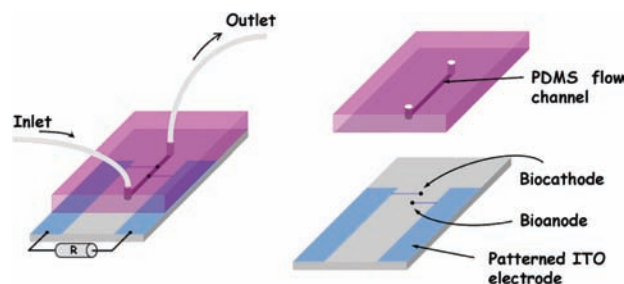

Scheme 2. Schematic Illustration of the Fabrication Procedure for the Bioanode and Biocathode of the BFC Logically Controlled by Aptamer-Based Biochemical Signals (Enzymes: GOD for the Bioanode and BOD for the Biocathode)
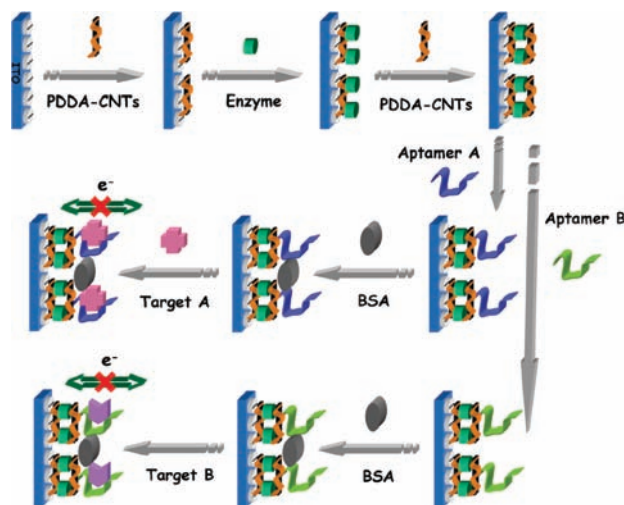
The BFC logically controlled by an aptamer system was composed of two on-chip patterned indium tin oxide (ITO) electrodes (Scheme 1) modified with an enzyme/aptamer-based self-assembled multilayer consisting of poly(diallyldimethylammonium chloride)-wrapped carbon nanotubes (PDDA-CNTs), enzyme [glucose oxidase (GOD) for the bioanode and bilirubin oxidase (BOD) for the biocathode], aptamer, and bovine serum albumin (BSA) (Scheme 2) [for details, see the Supporting Information (SI)]. By assembly of the as-prepared GOD/aptamer-based bioanode and BOD/aptamer-based biocathode to form a microchip-based compartmentless glucose/O₂ BFC, the fabricated BFC operates in an air-saturated base solution [i.e., air-saturated pH 7.4 Tris-HCl buffer (20 mM Tris-HCl, 140 mM NaCl, 5 mM KCl, 5 mM MgCl₂)] containing 20 mM glucose as the fuel and 0.5 M ferrocene monocarboxylic acid (FMCA) as the diffusional redox mediator helping GOD oxidize glucose fuel and BOD reduce O₂ oxidizer

(Scheme 3). In order to demonstrate the concept of "mutual benefits" between aptamers and BFCs, thrombin-binding aptamer and lysozyme-binding aptamer were chosen as the *proof-of-concept aptamers* applied in this work.

Scheme 3. Schematic Illustration of the Assembled Aptamer-Based BFC Logically Controlled by Biochemical Signals That Mimicks a Boolean **NAND** Logic Gate
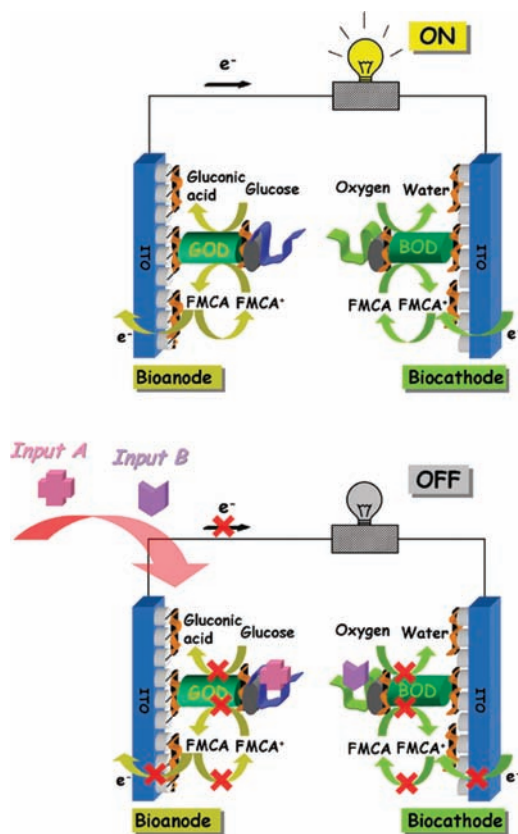
The aptamer-based biochemical-signal-controlled BFC mimicking a Boolean **NAND** logic gate was composed of a GOD/thrombin-binding aptamer-based bioanode and a BOD/lysozyme-binding aptamer-based biocathode (Scheme 3). Atomic force microscopy (AFM) was used to monitor the fabrication process of the bioanode and biocathode (Figures S1 and S2 in the SI). Control experiments suggested that GOD and BOD immobilized in the multilayer played an important role in glucose oxidation at the bioanode and O_2 reduction at the biocathode, respectively (Figures S3 and S4 in the SI). In order to perform the logic operations, the absence of thrombin [**Input A** (8 nM)] or lysozyme [**Input B** (20 nM)]) was considered as input **0**, while their presence at the operational concentrations was considered as input **1**. We also defined the open-circuit potential of the BFC as output **1** when it was above the threshold of 0.05 V and output **0** when it was below 0.05 V. In the presence of thrombin only [input (**1,0**)], thrombin-binding aptamer on the outermost layer of the self-assembled multilayer on the bioanode would catch thrombin and block the electrode interface (Scheme 3), resulting in an increase in the onset potential for glucose oxidation at the bioanode from ~0.20 to ~0.32 V [input (**1,0**) in Figure 1A]. However, the presence of thrombin did not obviously change the electrocatalytic activity of the BOD/lysozyme-binding aptamer-based biocathode toward O_2 reduction [input (**1,0**) in Figure 1A] because of the specificity of lysozyme-binding aptamer. Thus, the (**1,0**) input made the open-circuit potential of the BFC decrease to ~0.18 V [input (**1,0**) in Figure 1B]. In addition, also on the basis

of the specificity of the aptamer, the presence of lysozyme can only make the aptamer-target recognization occur at the BOD/lysozyme-binding aptamer-based biocathode, leading to an onset potential of ~0.34 V at the biocathode for O_2 reduction [input (**0,1**) in Figure 1A]; accordingly, the open-circuit potential decreased to ~0.14 V [input (**0,1**) in Figure 1B]. In the presence of both substrates [input (**1,1**)], aptamer-target recognization occurred at both the bioanode (between thrombin-binding aptamer and thrombin) and biocathode (between lysozyme-binding aptamer and lysozyme), and the onset potentials for the bioanode and biocathode reached ~0.32 and ~0.34 V, respectively [input (**1,1**) in Figure 1A]; consequently, the open-circuit potential decreased to ~0.02 V [input (**1,1**) in Figure 1B]. Furthermore, application of the (**0,0**) input did not obviously change the open-circuit potential of the BFC [input (**0,0**) in Figure 1B]. Therefore, the features of the system correspond to the equivalent circuitry of a **NAND** logic gate performing the Boolean logic operation of $A' + B'$ (Figure 1C−E). In addition to the dependence of the power density on the open-circuit potential of the BFC upon different input signals as mentioned above (Figure 1B), the dependence of the power density on the BFC current density was also investigated (Figure S5 in the SI).

NAND logic is represented by the situation where the output of the gate is inhibited only when both inputs are present (Figure 1C−E). Thus, in the presence of both thrombin and lysozyme inputs in a sample [input (**1,1**)], the open-circuit potential is significantly reduced (output **0**), and the **NAND** gate switches **OFF**. If one [input (**0,1**) or (**1,0**)] or neither [input (**0,0**)] of the analytes is present in the sample, the open-circuit potential is still "activated" (output
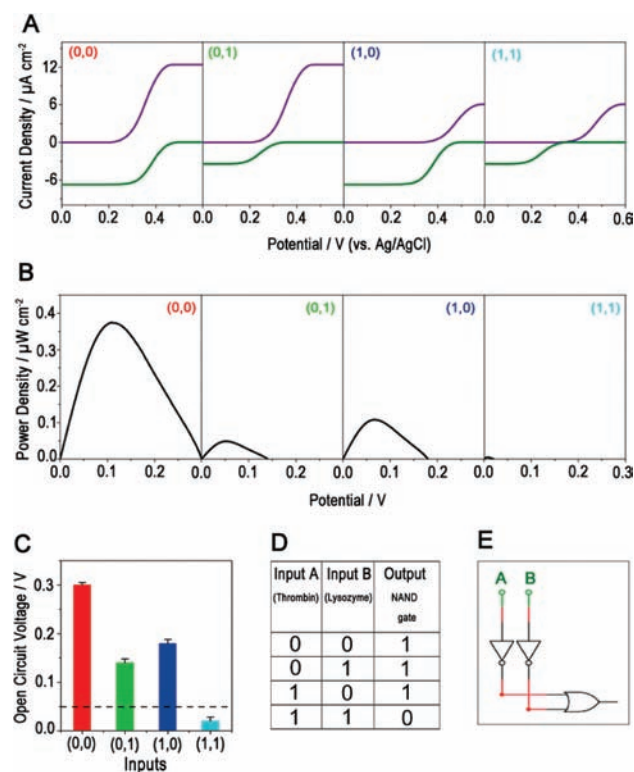
Figure 1. (A) Polarization curves of the bioanode (violet curves) and biocathode (olive curves) after the input signals (**0,0**), (**0,1**), (**1,0**), and (**1,1**). Scan rate: 0.1 mV s⁻¹. (B) Dependence of the power density on the BFC voltage after the input signals (**0,0**), (**0,1**), (**1,0**), and (**1,1**). Scan rate: 0.1 mV s⁻¹. (C) Bar diagram showing the open-circuit potential of the BFC for different combinations of input signals, derived from Figure 1B. The dashed line shows the threshold (0.05 V). (D) Truth table for a **NAND** logic gate. (E) Circuit for a **NAND** logic gate. **Input A**: 8 nM thrombin. **Input B**: 20 nM lysozyme.

1). Thus, the **NAND** logic gate presented here queries two target biological species in a sample to determine in a single test whether they are both present.

It should be noted that as the target concentrations increased, the overpotentials for glucose oxidation at the bioanode and O_2 reduction at the biocathode for the proposed **NAND** logic system gradually increased until the target concentrations reached "saturated concentrations" (Figure 2). Accordingly, the open-circuit potential of the BFC would not stop decreasing until the target concentrations in the sample got to their saturated concentrations. Thus, we optimized the saturated concentration as the input concentration for each input (i.e., 8 nM for thrombin and 20 nM for lysozyme according to the experimental results in Figure 2). We believe that such a saturated concentration assigned to the nature of the aptamer-based electrode would be important for constructing accurate and intelligent Boolean logic aptasensors or related bioelectronic devices. In addition, in this work, we used FMCA as the diffusional redox mediator in both the bioanodic and biocathodic reactions of the BFC, which would limit the voltage generated by the BFC. However, this problem can be solved by fabricating a compart-mentless BFC with different immobilized mediators on the bioanode and biocathode, and such an aptamer-controlled BFC system can also operate as a **NAND** logic gate (Scheme S2 and Figures S6−S8 in the SI).
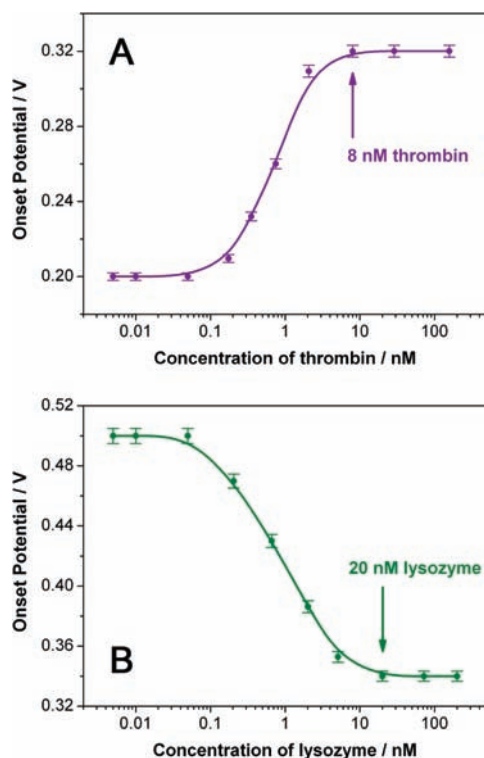
In conclusion, for the first time, we have introduced aptamer logic systems into BFCs to control the power release of the BFCs. Such integration may not only give us an avenue to control BFC power release by aptamer-based biocomputing systems but also indicate an interesting concept of "mutual benefits" between aptamers and BFCs, i.e., utilizing aptamer-based biochemical signals in the logic operation for controlling the BFCs' power release and applying the BFCs as self-powered and intelligent biosensors for logic aptasensing. In contrast to traditional biosensors, the fabricated logic aptasensors are self-powered, smart, and able to sense whether both specific targets are present by using the built-in Boolean logic. The proof-of-concept pattern of thrombin and lysozyme inputs to the open-circuit potential of the BFC outputs executed according to the truth table for a **NAND** gate also demonstrates the feasibility of performing self-powered medical diagnostics using logic-gate design. If we apply *pathologically related target-binding aptamers* into the aptamer logic-system-controlled BFCs,[7] one possible application of such logic systems could involve performing self-powered smart diagnostics, which would be direct screening of various medical conditions that are dependent on combinations of diagnostic aptamers.[7] It also should be noted that aptamers exhibit many unprecedented advantages in comparison with antibodies (i.e., immune system) or other biomimetic receptors,[6] including a wide range of targets (ranging from proteins to peptides, amino acids, drugs, metal ions, and even whole cells), comparable or even better target affinity, easy and cost-effective synthesis with high reproduc-ibility and purity, simple and straightforward chemical modification, etc. Thus, the aptamer logic systems proposed in this work would have their inherent and unique characteristics.

Supporting Information Available: Additional information as noted in the text. This material is available free of charge via the Internet at http://pubs.acs.org.

Figure 2. (A) Onset potentials for glucose oxidation at the GOD/thrombin-binding aptamer-based bioanode for different concentrations of thrombin. As indicated by the arrow, the saturated concentration for thrombin is 8 nM. (B) Onset potentials for oxygen reduction at the BOD/lysozyme-binding aptamer-based biocathode for different concentrations of lysozyme. As indicated by the arrow, the saturated concentration for lysozyme is 20 nM.

References

(1) (a) Barton, S. C.; Gallaway, J.; Atanassov, P. *Chem. Rev.* **2004**, *104*, 4867–4886. (b) Heller, A. *Anal. Bioanal. Chem.* **2006**, *385*, 469–473. (c) Cracknell, J. A.; Vincent, K. A.; Armstrong, F. A. *Chem. Rev.* **2008**, *108*, 2439–2461. (d) Moehlenbrock, M. J.; Minteer, S. D. *Chem. Soc. Rev.* **2008**, *37*, 1188–1196.
(2) Logan, B. E.; Hamelers, B.; Rozendal, R.; Schroder, U.; Keller, J.; Freguia, S.; Aelterman, P.; Verstraete, W.; Rabaey, K. *Environ. Sci. Technol.* **2006**, *40*, 5181–5192.
(3) (a) Amir, L.; Tam, T. K.; Pita, M.; Meijler, M. M.; Alfonta, L.; Katz, E. *J. Am. Chem. Soc.* **2009**, *131*, 826–832. (b) Tam, T. K.; Strack, G.; Pita, M.; Katz, E. *J. Am. Chem. Soc.* **2009**, *131*, 11670–11671.
(4) (a) Stojanovic, M. N.; Stefanovic, D. *J. Am. Chem. Soc.* **2003**, *125*, 6673–6676. (b) Saghatelian, A.; Volcker, N. H.; Guckian, K. M.; Lin, V. S. Y.; Ghadiri, M. R. *J. Am. Chem. Soc.* **2003**, *125*, 346–347. (c) Kolpashchikov, D. M.; Stojanovic, M. N. *J. Am. Chem. Soc.* **2005**, *127*, 11348–11351.
(5) (a) Niazov, T.; Baron, R.; Katz, E.; Lioubashevski, O.; Willner, I. *Proc. Natl. Acad. Sci. U.S.A.* **2006**, *103*, 17160–17163. (b) Muramatsu, S.; Kinbara, K.; Taguchi, H.; Ishii, N.; Aida, T. *J. Am. Chem. Soc.* **2006**, *128*, 3764–3769. (c) Strack, G.; Ornatska, M.; Pita, M.; Katz, E. *J. Am. Chem. Soc.* **2008**, *130*, 4234–4235.
(6) (a) Famulok, M.; Hartig, J. S.; Mayer, G. *Chem. Rev.* **2007**, *107*, 3715–3743. (b) Tombelli, S.; Mascini, M. *Curr. Opin. Mol. Ther.* **2009**, *11*, 179–188. (c) Liu, J.; Cao, Z.; Lu, Y. *Chem. Rev.* **2009**, *109*, 1948–1998. (d) Sefah, K.; Phillips, J. A.; Xiong, X.; Meng, L.; Simaeys, D. V.; Chen, H.; Martin, J.; Tan, W. *Analyst* **2009**, *134*, 1765–1775.
(7) Konry, T.; Walt, D. R. *J. Am. Chem. Soc.* **2009**, *131*, 13232–13233.

JA910634E